



# Sympathetic nerve tissue in milky spots of the human greater omentum

Cindy G. J. Cleypool  Bernadette Schurink,  Dorinde E. M. van der Horst and Ronald L. A. W. Bleys

Department of Anatomy, Division of Surgical Specialties, University Medical Center Utrecht, Utrecht University, Utrecht, The Netherlands

## Abstract

Omental milky spots (OMSs), small lymphoid structures positioned in the greater omentum, are involved in peritoneal immune homeostasis and the formation of omental metastases. Sympathetic nerve activity is known to regulate immune function in other lymphoid organs (e.g. spleen and lymph nodes) and to create a favourable microenvironment for various tumour types. However, it is still unknown whether OMSs receive sympathetic innervation. Therefore, the aim of this study was to establish whether OMSs of the adult human greater omentum receive sympathetic innervation. A total of 18 OMSs were isolated from five omenta, which were removed from 3% formaldehyde-perfused cadavers (with a median age of 84 years, ranging from 64 to 94). OMSs were embedded in paraffin, cut and stained with a general (PGP9.5) and sympathetic nerve marker (TH and DBH), and evaluated by bright field microscopy. A T-cell, B-cell, and macrophage staining was performed to confirm OMS identity. In 50% of the studied OMSs, sympathetic nerve fibres were observed at multiple levels of the same OMS. Nerve fibres were represented as dots or elongated structures and often observed in relation to small vessels and occasionally as individual structures residing between lymphoid cells. The current study shows that 50% of the investigated OMSs contain sympathetic nerve fibres. These findings may contribute to our understanding of neural regulation of peritoneal immune response and the involvement of OMSs in omental metastases.

**Key words:** greater omentum; innervation; metastases; neuroimmunomodulation; omental milky spot; sympathetic.

## Introduction

Body cavities are lined by mesothelium and the sub-mesothelial compartment of the pleura, pericardium, and peritoneum (both parietal and visceral) is known to contain lymphoid cell clusters, referred to as milky spots (MSs) (Michailova & Usunoff, 2004). The most prominently present and extensively studied MSs are the ones positioned in the omentum, hence referred to as omental MSs (OMSs). OMSs are cellular aggregates of macrophages, B-cells, and T-cells (Shimotsuma et al. 1991; Liu et al. 2015). They develop during ontogeny (Krist et al. 1997), are found in

various animal species including humans (Michailova & Usunoff, 2004), and can be observed in large fixed omental tissue samples after staining with haematoxylin (Schurink et al. 2019) (Fig. 1). OMSs play an important role in the peritoneal immune response: (1) peritoneal fluid is absorbed via openings (stomata) in the omental mesothelial lining and is monitored in OMSs for foreign or pathogenic substances (Van Vugt et al. 1996; Wilkosz et al. 2005; Mezaperez & Randall, 2017), and (2) OMSs form a gateway for circulating immune cells that are recruited towards the peritoneal cavity during a peritoneal immune challenge (Wijffels et al. 1992). In addition, OMSs are involved in peritoneal metastatic disease; they form primary implantation sites for peritoneal exfoliated cancer cells, which can develop into omental metastases (Krist et al. 1998; Hagiwara et al. 1993; Tsujimoto et al. 1995, 1996).

The autonomic nervous system, and in particular sympathetic nerves, are known to be involved in local regulation of the immune response in lymphoid organs, such as the spleen and lymph nodes (Mignini et al. 2003; Komegae et al. 2018), and in creating a tumour-stimulating microenvironment (Cole et al. 2015). So far only a few studies have

### Correspondence

Cindy G. J. Cleypool and Ronald L. A. W. Bleys, University Medical Center Utrecht, Division of Surgical Specialties, Department of Anatomy, Universiteitsweg 100, P.O. Box 85060, 3508 AB Utrecht, the Netherlands. (C.G.J.C.) T: + 31 (0)88 7568317; E: c.g.j.cleypool@umcutrecht.nl; (R.L.A.W.B.) T: + 31 (0)88 7568302; F: + 31 (0)88 7569030; E: r.l.a.w.bleys@umcutrecht.nl

†These authors contributed equally to the work.

Accepted for publication 30 July 2019

Article published online 9 September 2019

reported on OMS-associated nerve fibres (Krist et al. 1994; Havrlentova et al. 2017; Yildirim et al. 2010) but none of these have addressed sympathetic fibres specifically. If, like other lymphoid structures, OMSs receive sympathetic innervation, this nerve tissue, or its effectors, could hold potential as therapeutic targets to modify peritoneal immune response or tumor environment. Therefore, the aim of this study is to establish whether OMSs of the adult human greater omentum receive sympathetic innervation.

## Methods

The greater omenta of five human cadavers were studied. These included three male and two female cadavers with a median age of 84, ranging from 64 to 94 years. Bodies were donated through a body donation programme to the Anatomy Department of the University Medical Center Utrecht, the Netherlands. Informed consent was obtained during life, allowing the use of these bodies for educational and research purposes. No scars were observed in the abdominal region and the available medical records did not list relevant diseases such as cancerous, immune or neurodegenerative disease.

Whole body preservation was accomplished by perfusion with 3% formaldehyde via the femoral artery. The aprons of the omenta were resected from the transverse colon and stored in a 0.1 M phosphate buffer, pH 7.4, containing 15% sucrose [phosphate-buffered saline (PBS)/sucrose] at 4 °C until further investigation. One or two large samples of approximately 6 × 4 cm were removed from each

omentum. These samples were stained with haematoxylin (Schurink et al. 2019) and evaluated for the presence of OMSs with the aid of a stereomicroscope (Leica EZ4, Nussloch, Germany), using both transmission and incident light. OMSs were identified, removed (with a small margin of surrounding tissue), and placed in PBS/sucrose at 4 °C until further processing for microscopic investigation. As it is known that sympathetic nerve fibres accompany arteries towards their end organs (Mitchel, 1956), omental arterial branches were studied to verify the presence of sympathetic nerve fibres in the selected omental regions. Figure 2 contains schematic images of the selected omental regions, and the amount of isolated OMSs and arterial branches per investigated omentum.

## Immunohistochemistry

MSs and omental arteries were processed for paraffin embedding by placing them in increasing percentages of ethanol, xylene, and paraffin. Paraffin blocks were cut on a microtome (Leica 2050 Super Cut, Nussloch, Germany) and 5- $\mu$ m-thick sections were placed on glass slides, air-dried, and subsequently heat-fixed for 2 h on a slide drying table of 60 °C (Medax, 14801, Kiel, Germany). Each OMS was serially cut and slides were selected at multiple levels for microscopic investigation. Adjacent slides of each OMS level and of each omental artery were stained with antibodies against general [protein gene product 9.5 (PGP9.5)] and sympathetic [tyrosine hydroxylase (TH) and dopamine beta-hydroxylase (DBH)] nerve tissue. If comparable staining patterns were present in TH- and DBH-stained samples, it was assumed that immunoreactive (IR) tissue represented sympathetic nerve tissue. To confirm OMS identity,

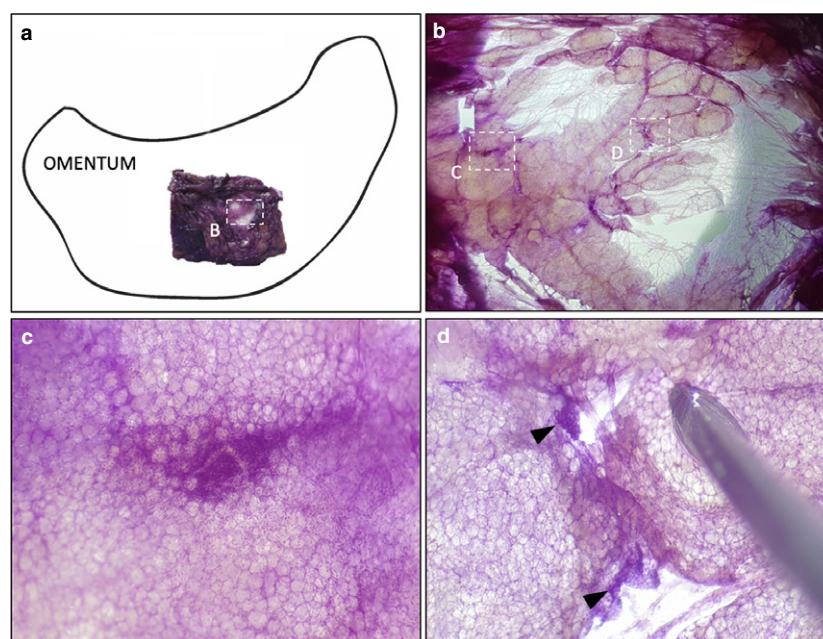


**Fig. 1** Haematoxylin-stained fixed human greater omentum. After selection and haematoxylin staining of a large omental sample, omental milky spots (OMSs) can be observed when studied through a stereomicroscope. (a) Schematic drawing of an omentum showing a stained area. The boxed region represents an OMS-rich area that is magnified in (B). (b) Stereomicroscopic image of a haematoxylin-stained omental sample. The omental tissue contains translucent areas and areas with fat pads composed of lobules of adipose tissue. Dark-stained areas represent cell dense regions (nuclei are stained dark blue by haematoxylin). (c,d) Magnifications of region (C and D) of (b). When magnified, some dark-stained areas contained dense clusters of cells with moderate-size round nuclei. (c) A moderately sized OMS composed of a clusters of lymphoid cells positioned superficial to adipocytes. A vascular structure runs through the OMS. (d) Two smaller OMSs (black arrowheads).

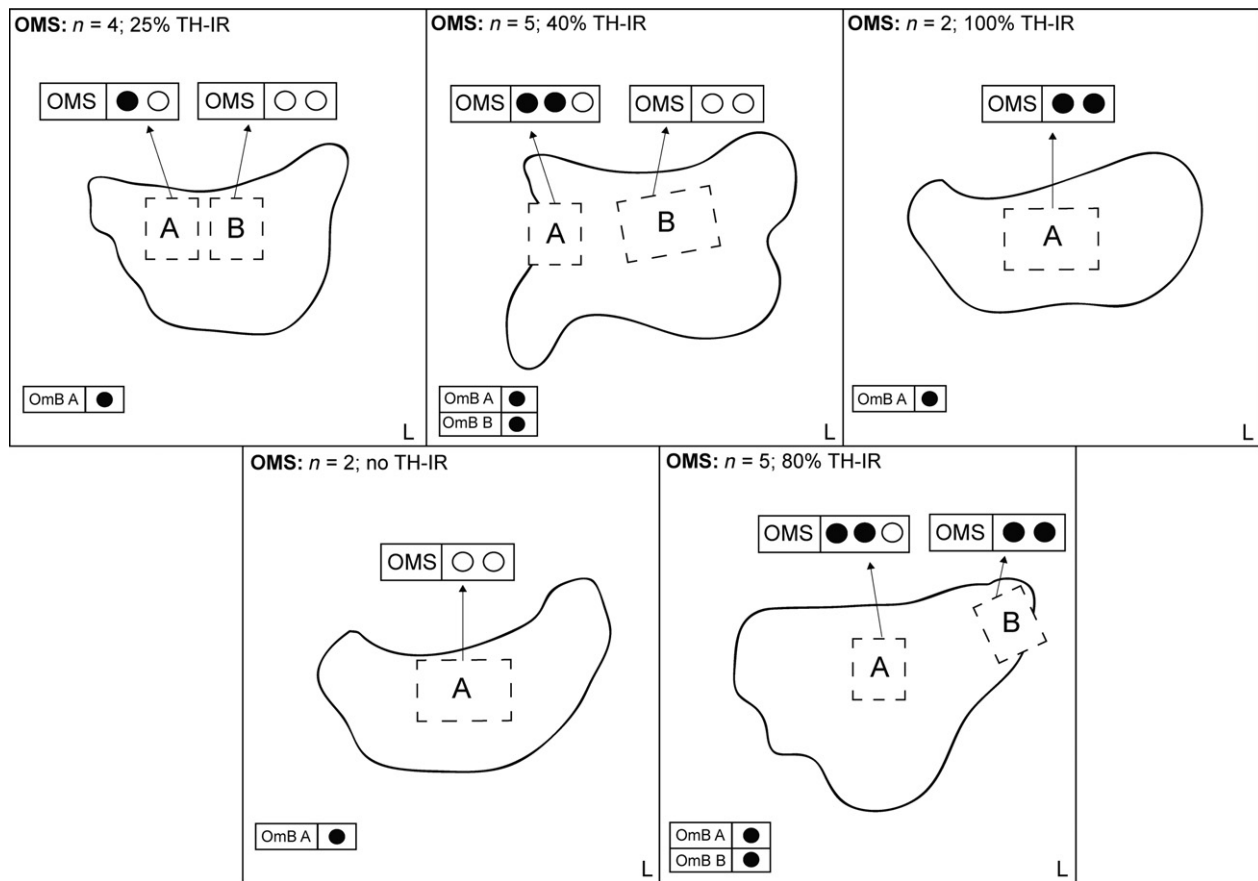


**Fig. 2** Schematic representation of studied human greater omenta. The selected regions of each omentum are boxed and marked (A or B). Per region, the number of omental milky spots (OMSs) is depicted by dots (black dots represent OMSs with TH-immune reactive [IR] nerve fibres). In the left upper corner of each frame, the number of stained OMSs is listed, including the percentage of OMSs with TH-IR nerve fibres. In the left lower corner of each frame, the number of studied omental arterial branches is depicted as dots (black dots represent omental branches with TH-IR nerve fibres). n, number.

additional slides were stained for the presence of B-cells (CD20), T-cells (CD3), and macrophages (CD68), the main cellular constituents of human OMSs (Shimotsu et al. 1991; Liu et al. 2015). As sympathetic regulation of splenic immune function is known primarily to involve adrenergic activation of T-helper cells (Kin & Sanders, 2006; Olofsson et al. 2012), an additional CD4 antibody staining was performed. All slides were deparaffinized and rehydrated, followed by 20 min of antigen retrieval in 95 °C citrate buffer on a hot plate. After washing in Tris-buffered saline (TBS) with 0.05% Tween (TBS/Tween), sections were pre-incubated for 10 min with 5% normal human or goat serum, with the exception of the ones selected for CD68 staining. After pre-incubation, sections were incubated with primary antibodies in TBS with 3% bovine serum albumin. Table 1 contains details of the primary antibodies. Following incubation, sections were washed with TBS/Tween and incubated for 30 min at room temperature (RT) with undiluted Brightvision Poly-Alkaline phosphatase Goat-anti-Rabbit (ImmunoLogic, Amsterdam, the Netherlands) in the case of PGP9.5, TH, DBH and CD3 staining, or Brightvision Poly-Alkaline phosphatase Goat-anti-Mouse (ImmunoLogic) in the case of CD20, CD68 and CD4 staining. After incubation with secondary antibodies, all sections were washed with TBS and incubated with Liquid Permanent Red (LPR; Dako, Glostrup, Denmark) for 10 min. Subsequently, tissue sections were washed with distilled water and counterstained with haematoxylin, air-dried at

60 °C for 90 min, and coverslipped using Entellan (Merck, Darmstadt, Germany). Human sympathetic trunk sections were included as positive controls for all three nerve markers and human spleen sections for all four immune cell markers. Negative controls were obtained by incubation of sympathetic trunk, spleen, and OMSs slides with TBS-3% bovine serum albumin without primary antibodies. All slides were evaluated using bright field microscopy.

### Image acquisition

Brightfield single images were captured at various magnifications using a DM6 microscope with a motorized scanning stage, a DFC7000 T camera, and LASX software (all from Leica).

### Results

OMSs could be identified in haematoxylin-stained omental samples of all five cadavers, according to a previous description (Schurink et al. 2019). Of the five studied omenta, 18 OMSs (2–5 per omentum) and 7 omental arterial branches (1–2 per omentum) were sampled and processed for microscopic evaluation. All positive controls

**Table 1** Primary antibodies

Primary antibody	Clone	Manufacturer	Reference number	Dilution	Incubation time	Temperature	Pre-incubation serum	
PGP9.5	Polyclonal rabbit anti-human	n.a.	Dako, Denmark	Z5116	1 : 2000	48 h	4	5% NHS
TH	Polyclonal rabbit anti-human	n.a.	Pelfreeze, USA	P40101	1 : 1500	12 h	RT	5% NHS
DBH	Monoclonal rabbit anti-human	EPR20385	Abcam, UK	AB209487	1 : 1000	12 h	RT	5% NHS
CD68	Monoclonal mouse anti-human	514H12	NovoCastr, UK	NCL-L-CD68	1 : 25	12 h	RT	NO pre-incubation
CD20	Monoclonal mouse anti-human	L26	Dako, Denmark	M0755	1 : 400	60 min	RT	5% NHS
CD3	Polyclonal mouse anti-human	n.a.	Dako, Denmark	A0452	1 : 50	90 min	RT	5% NGS
CD4	Monoclonal mouse anti-human	4B12	Dako, Denmark	M7310	1 : 25	120 min	RT	5% NGS

showed expected IR patterns, whereas all negative controls were clean.

### Omental milky spots

All 18 selected OMSs showed specific microscopic morphological OMS features. They were composed of clusters of lymphoid cells, contained blood vessels, and were surrounded by adipose tissue (Shimotsuma et al. 1989; Wilkosz et al. 2005; Liu et al. 2015; Meza-Perez & Randall, 2017). The median diameter of these OMSs was 379  $\mu\text{m}$ , ranging from 139 to 1150  $\mu\text{m}$ . TH-IR was present in nine of 18 OMSs (50%). Figure 2 contains schematic drawings of the investigated omenta including the number of studied OMSs and whether they contained sympathetic nerve fibres. Four of five omenta contained TH-IR fibres in 25–100% of their investigated OMSs. Only one cadaver showed no TH-IR fibres in any of its OMSs. TH-IR in OMSs was observed as individual small spots (Fig. 3A-F) or as elongated structures with a dotted appearance resembling varicosities (encircled structures in Fig. 3B). In all TH-IR OMSs, immune labelling was observed at all studied levels of the same OMSs and in comparable regions. TH-IR structures were often closely related to small OMS blood vessels but were also present as individual structures in close proximity to lymphoid cells (Fig. 3). TH-IR patterns were highly comparable with PGP9.5-IR patterns, suggesting that TH-IR represented neural structures. TH-IR patterns were comparable to DBH-IR patterns. Therefore, it was confirmed that these neural structures were adrenergic and not dopaminergic.

### Immune cells

All OMSs were composed of B-cells, T-cells, and macrophages, confirming their OMS identity (Fig. 4B-D). CD4 staining was performed on slides of all TH-IR OMSs and

CD4-positive cells were clearly present and distributed homogeneously in three of four cadavers with TH-IR OMSs (Fig. 4E). In one cadaver, no CD4-IR cells could be observed in any of the three TH-IR OMSs.

### Omental branches

From each of the five cadavers, one or two omental arterial branches were studied, resulting in a total number of seven branches. PGP 9.5-, TH-, and DBH-staining showed comparable patterns and sympathetic nerve fibres were observed in all studied omental arterial branch samples, either as discrete fibres or in bundles. Discrete nerve fibres were present in the adventitia up to the level of the adventitial-medial border in all omental branches, representing intrinsic vessel wall innervation (Fig. 5A,B). In five of seven omental arterial branches, nerve bundles were observed in the adventitia or surrounding connective tissue, representing nerve fibres accompanying these arteries towards more distal omental structures (Fig. 5A,B).

### Discussion

This study shows that human omental OMSs contain sympathetic nerve fibres. Often, these nerve fibres were located around small blood vessels and occasionally, individual nerve fibres were observed between lymphoid cells. By means of TH, confirmed by DBH staining, sympathetic fibres were observed in 50% of the studied OMSs. The absence of TH-IR inside the other OMSs is not likely to be explained by either poor or excessive formaldehyde fixation, as TH-IR fibres and bundles have been observed in tissue surrounding these OMSs and omental arterial branches. An age-related decrease of sympathetic tissue in OMS of our relatively old study subjects (median age of 84 years) would be a more plausible explanation, as sympathetic nerve



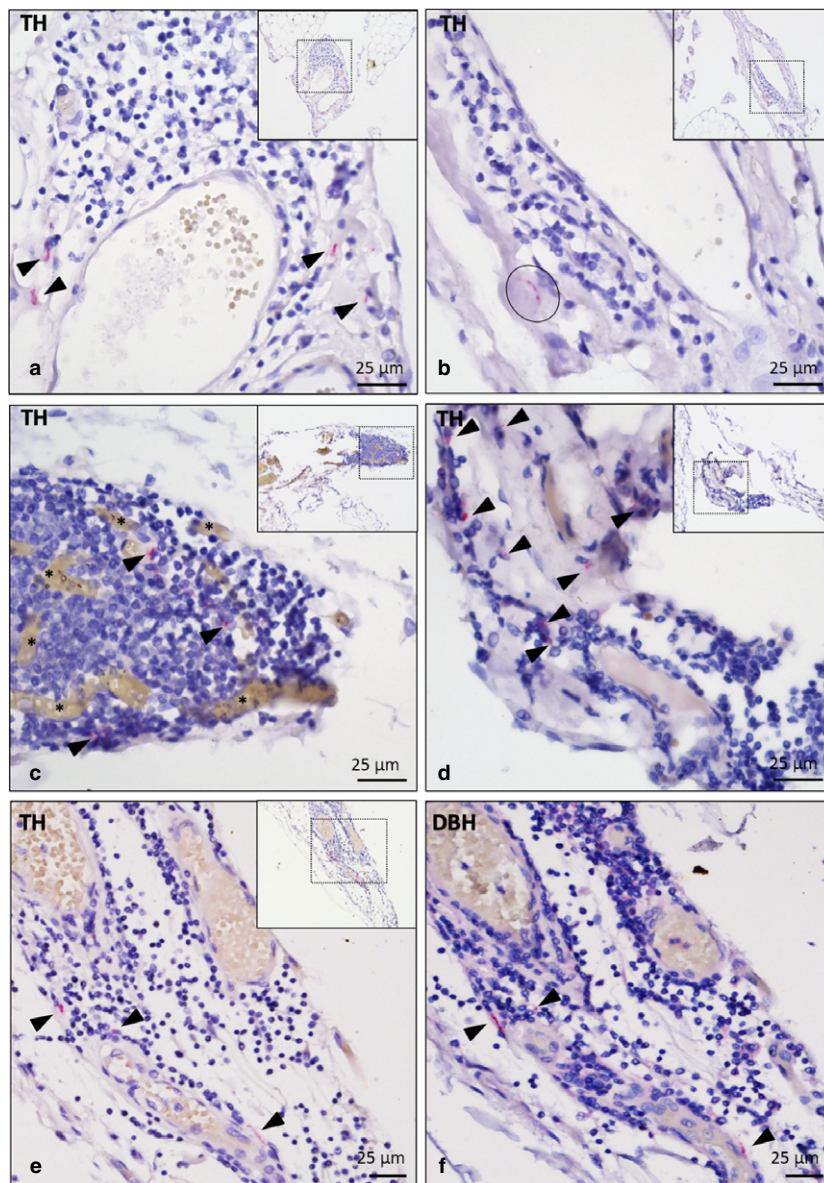


**Fig. 3** Sympathetic nerve structures in different omental milky spots. Each image contains an inlay with an overview image of the omental milky spot (OMS) and its surroundings. TH-IR structures are stained pink (indicated with black arrowheads) and cell nuclei are stained dark blue. (a) OMS of a male cadaver of 94 years of age. TH-immune reactive (IR) structures can be observed as discrete structures or in close proximity to immune cells. (b) OMS of a male cadaver of 94 years of age. An elongated TH-IR structure (encircled), with a dotted appearance, most likely representing varicosities, is present in close proximity to immune cells of the OMS. (c) OMS with a high cell density of a female cadaver of 84 years of age. Many vascular structures can be observed within the OMS (asterisk). TH-IR structures were observed primarily in close proximity to immune cells. (d) OMS of a female cadaver of 84 years of age. Few TH-IR structures can be observed, in close proximity to lymphocytes. (e) MS of a male cadaver of 88 years of age. TH-IR structures were observed in relation to a blood vessel, but small TH-IR structures were in close proximity to immune cells as well. (f) The same OMS as in (e) but stained for DBH. Staining patterns of (e) and (f) are comparable, supporting the fact that TH-IR structures represent sympathetic nerve tissue.

tissue of secondary lymphoid structures is known to decline with age (Bellinger et al. 1992).

So far, only three other studies have described nerve tissue associated with OMSs. In two of these studies a general nerve marker (S-100) was used and the type of nerve tissue was not further specified (Havrlentova et al. 2017; Yildirim

et al. 2010). Although these studies visualized small S-100-IR nerve bundles closely related to blood vessels, in between adipocytes or in the surrounding connective tissue, they do not describe small neural structures in close proximity to lymphoid cells. This in contrast to the results of the current study, in which fibres were observed in relation with

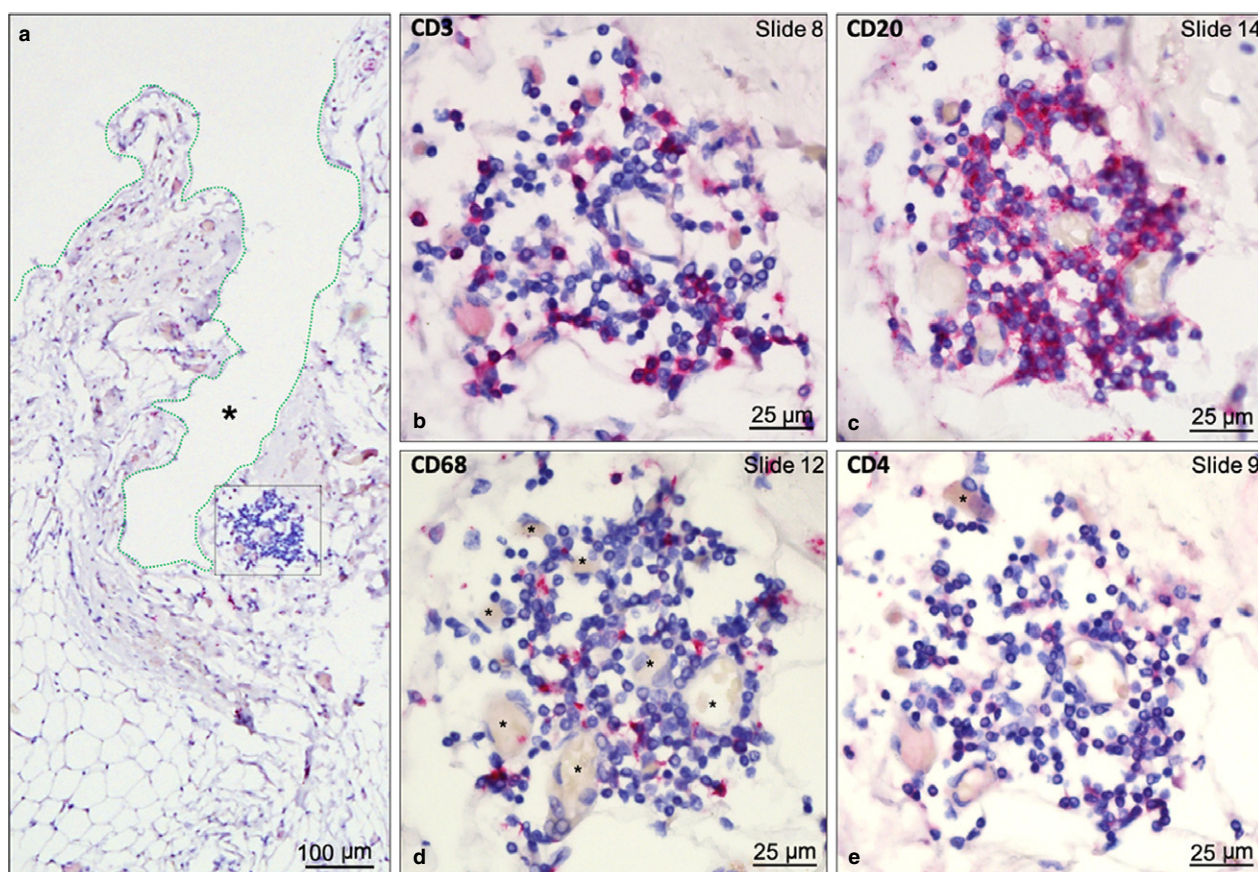


**Fig. 4** Presence of immune cells in an omental milky spot. The panel is composed of images of the same omental milky spot (OMS) stained for various immune cells. (a) Overview image of omental tissue containing an OMS (cell-dense region in boxed area) with surrounding adipose tissue. The OMS is positioned directly underneath the mesothelial lining (green dotted line) of the omentum. The abdominal cavity is marked with a large black asterisk. Additional slides were stained to visualize (b) T-cells (CD3), (c) B-cells (CD20), (d) macrophages (CD68), and (e) T-helper cells (CD4). IR structures are stained bright pink and cell nuclei are stained dark blue. Small vascular structures can be discriminated inside the OMS by the presence of erythrocytes which give the vessel lumina a brownish colour (as shown with small black asterisks in d).

lymphocytes. The third study used transmission electron microscopy in combination with a dopamine (DA) marker to study innervation of OMSs in two patients under the age of 28 years with unaffected omenta. The authors observed non-myelinated nerve fibres in the OMSs of both subjects (Krist et al. 1994). These nerve fibres contained DA-IR vesicles and the authors concluded that the fibres were dopaminergic. However, DA is a precursor for NA and the nerve tissue could represent both dopaminergic and noradrenergic fibres. In the current study the commonly accepted adrenergic nerve marker TH and a marker for dopamine beta-hydroxylase (DBH), the enzyme involved in conversion of DA to NA, were used on adjacent slides of both OMSs and omental arterial branches. TH staining patterns were comparable to DBH staining patterns, suggesting the present nerve tissue to be adrenergic. However, as no double staining was performed, the presence of dopaminergic fibres could not be excluded. Furthermore, the transmission electron microscopic study of Krist et al. (1994) revealed non-myelinated nerve endings to be in

close proximity to immune cells (Krist et al. 1994), a finding which is in line with the results of the current study. Previously, this finding led to the suggestion that these nerves might modulate immune cell function by the release of their neurotransmitter. The suggestion that this nerve tissue could modify immune cell function is highly interesting because it opens new opportunities for anti-inflammatory therapies. The concept of neural structures modifying immune function is known as neuroimmunomodulation. It is acknowledged that the sympathetic nervous system plays an important role in regulation of the systemic inflammatory response via the spleen (Komegae et al. 2018). Activation of sympathetic nerve tissue of the splenic plexus results in a cascade of intrasplenic events, starting with the release of norepinephrine (Kees et al. 2003), followed by adrenergic receptor activation on CD4-positive T-cells (Rosas-Ballina et al. 2011; Vida et al. 2011, 2017), which results in production and secretion of acetylcholine and ultimately inhibits the release of pro-inflammatory cytokines from activated macrophages (Borovikova et al. 2000; de



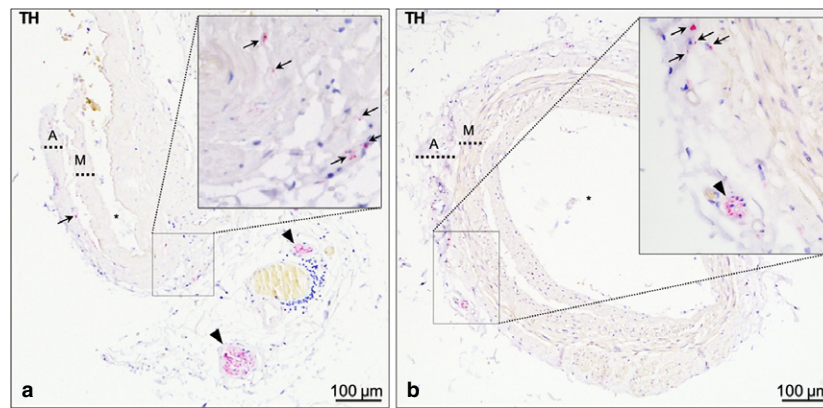


**Fig. 5** Omental arterial branches supplying areas of the greater omentum of which milky spots were selected for investigation. TH-immune reactive (IR) structures are stained pink and cell nuclei are stained dark blue. Both images (a,b) show an omental arterial branch with associated sympathetic nerve tissue. Paravascularly positioned nerve bundles (arrowheads) run with arteries towards their final destination. Discrete nerve fibres (arrows) innervate the blood vessel wall and can be observed in the adventitia up to the adventitial-medial border. (a) Omental arterial branch of a female cadaver of 84 years of age. (b) Omental arterial branch of a male cadaver of 88 years of age with a thickened intima. \*Blood vessel lumen; A, Tunica adventitia; M, Tunica media.

Jonge et al. 2005; Kox et al. 2009; Lu & Kwan, 2014). This results in dampening of the systemic inflammatory response. As OMSs are known to contain macrophages (Shimotsuma et al. 1991; Liu et al. 2015) and the current study shows that OMSs receive sympathetic innervation and contain CD4-positive T-cells, all required elements for neuroimmunomodulation appear to be present. Therefore, stimulation of sympathetic fibres of the greater omentum could result in dampening of the peritoneal immune response, which could be beneficial during peritoneal sepsis.

In addition to its possible role in neuroimmunomodulation, sympathetic innervation of OMSs might also be involved in the formation of peritoneal metastases. According to the seed and soil theory, as first proposed by Paget (1889), tumour cells (seeds) have a specific affinity for certain organs or structures (soil); metastasis would only develop if both seed and soil are compatible (Paget, 1889). MSs provide such a favourable soil for certain abdominal tumours (Hagiwara et al. 1993; Tsujimoto et al. 1995,1996; Krist et al. 1998). Why OMSs provide a hotspot for peritoneal metastases has not been fully elucidated yet. Previous studies have suggested a contributory role of OMS-specific mesothelium and blood vessels (Gerber et al. 2006) or adipocytes (Ladanyi et al. 2018). We propose an additional role for sympathetic innervation of OMSs. The sympathetic nerve system and specifically its neurotransmitter noradrenaline are known (1) to contribute to a favourable tumour microenvironment, for example by affecting stromal cells, endothelial cells, and tumour-associated macrophages (Magnon et al. 2013), and (2) to stimulate tumour cell proliferation, via beta ( $\beta$ ) adrenergic receptors on tumour cells (Coelho et al. 2017). As since all of these processes are mediated via adrenergic receptors, the effects of  $\beta$  adrenergic blocking as a potential anti-

tumour therapy have been investigated in *in vitro*, animal, and retrospective patient studies with promising results (Magnon et al. 2013; Coelho et al. 2017; Zahalka et al. 2017). Although further studies are needed to elucidate the exact anti-tumour mechanism, these findings suggest a potential role for  $\beta$ -blockers in the treatment of cancer. As a potential therapeutic application,  $\beta$ -blockers could be administered to the peritoneal cavity, discretely or as an adjuvant in hyperthermic intraperitoneal chemotherapy, which might limit or prevent intraperitoneal spread and growth of tumour cells.

To elucidate the role of sympathetic innervation of OMSs in the peritoneal immune response and metastatic disease, and its therapeutic potential, further studies are needed. These studies should include omenta from younger individuals to avoid age-related decrease of innervation and investigate the amount and location of sympathetic nerve tissue. Furthermore, these studies should investigate the (synaptic) relation of sympathetic nerve fibres to various OMS cell types such as immune and stromal cells, as well as the presence and type of adrenergic receptors on these cells. Although the current study focused on MSs in the greater omentum, similar structures, often referred to as extraomental MSs, can be found in the peritoneum, mesenterium, mediastinum, pericardium, and pleura (Michailova & Usunoff, 2004; Cruz-Migoni & Caamano, 2016). As these structures are involved in local immune activity (Cruz-Migoni & Caamano, 2016), including them in future studies is recommended.

In conclusion, this study showed that human OMSs are sympathetically innervated. Nerve fibres were observed in relation to both blood vessels and lymphocytes. The presence of sympathetic fibres in OMSs contributes to our understanding of how OMS immune function might be regulated during an abdominal immune challenge and why

they form primary implantation sites for peritoneal exfoliated cancer cells.

## Acknowledgements

We thank Suzanne Verlinde and Claire McKaaij of the Department of Anatomy of the University Medical Center Utrecht for their assistance in processing tissue samples and Evelien Kotte for her assistance with tissue collection.

## Authors' contributions

C.C. designed the study, interpreted the data, designed the figures, and wrote the manuscript. B.S. designed the study, interpreted the data, designed the figures, and wrote the manuscript. D.H. performed the experiments, and helped with the interpretation of the data and writing the manuscript. R.B. supervised the project and helped writing the manuscript.

## References

- Bellinger DL, Ackerman KD, Felten SY, et al. (1992) A longitudinal study of age-related loss of noradrenergic nerves and lymphoid cells in the rat spleen. *Exp Neurol* **116**, 295–311.
- Borovikova LV, Ivanova S, Zhang M, et al. (2000) Vagus nerve stimulation attenuates the systemic inflammatory response to endotoxin. *Nature* **405**, 458–462.
- Coelho M, Soares-Silva C, Brandão D, et al. (2017)  $\beta$ -Adrenergic modulation of cancer cell proliferation: available evidence and clinical perspectives. *J Cancer Res Clin Oncol* **143**, 275–291.
- Cole SW, Nagaraja AS, Lutgendorf SK, et al. (2015) Sympathetic nervous system regulation of the tumour microenvironment. *Nat Rev Cancer* **15**, 563–572.
- Cruz-Migoni S, Caamano J (2016) Fat-associated lymphoid clusters in inflammation and immunity. *Front Immunol* **7**, 1–7.
- Gerber SA, Rybalko VY, Bigelow CE, et al. (2006) Preferential attachment of peritoneal tumor metastases to omental immune aggregates and possible role of a unique vascular microenvironment in metastatic survival and growth. *Am J Pathol* **169**, 1739–1752.
- Hagiwara A, Takahashi T, Sawai K, et al. (1993) Milky spots as the implantation site for malignant cells in peritoneal dissemination in mice. *Cancer Res* **53**, 687–693.
- Havrlentova L, Faistova H, Mazur M, et al. (2017) Comparative analysis of human omental milky spots between the patients with colon cancer and the control group. *Bratisl Lek Listy* **118**, 580–584.
- de Jonge WJ, van der Zanden EP, The FO, et al. (2005) Stimulation of the vagus nerve attenuates macrophage activation by activating the Jak2-STAT3 signaling pathway. *Nat Immunol* **6**, 844–851.
- Kees M, Pongratz G, Kees F, et al. (2003) Via  $\beta$ -adrenoceptors, stimulation of extrasplenic sympathetic nerve fibers inhibits lipopolysaccharide-induced TNF secretion in perfused rat spleen. *J Neuroimmunol* **145**, 77–85.
- Kin NW, Sanders VM (2006) It takes nerve to tell T and B cells what to do. *J Leukoc Biol* **79**, 1093–1104.
- Komegae EN, Farmer DGS, Brooks VL, et al. (2018) Vagal afferent activation suppresses systemic inflammation via the splanchnic anti-inflammatory pathway. *Brain Behav Immun* **73**, 441–449.
- Kox M, van Velzen JF, Pompe JC, et al. (2009) GTS-21 inhibits pro-inflammatory cytokine release independent of the Toll-like receptor stimulated via a transcriptional mechanism involving JAK2 activation. *Biochem Pharmacol* **78**, 863–872.
- Krist LF, Eestermans IL, Steinbusch HW, et al. (1994) An ultrastructural study of dopamine immunoreactive nerve fibers in milky spots. *Neurosci Lett* **168**, 143–146.
- Krist LF, Koenen H, Calame W, et al. (1997) Ontogeny of milky spots in the human greater omentum: an immunochemical study. *Anat Rec* **249**, 399–404.
- Krist LF, Kerremans M, Broekhuis-Fluitsma DM, et al. (1998) Milky spots in the greater omentum are predominant sites of local tumour cell proliferation and accumulation in the peritoneal cavity. *Cancer Immunol Immunother* **47**, 205–212.
- Ladanyi A, Mukherjee A, Kenny H, et al. (2018) Adipocyte-induced CD36 expression drives ovarian cancer progression and metastasis. *Oncogene* **37**, 2285–2301.
- Liu JY, Yuan JP, Geng XF, et al. (2015) Morphological study and comprehensive cellular constituents of milky spots in the human omentum. *Int J Clin Exp Pathol* **8**, 12877–12884.
- Lu B, Kwan K (2014)  $\alpha 7$  nicotinic acetylcholine receptor signaling inhibits inflammasome activation by preventing mitochondrial DNA release. *Mol Med* **20**, 350–358.
- Magnon C, Hall SJ, Lin J, et al. (2013) Autonomic nerve development cancer progression. *Science* **341**, 1–10.
- Meza-Perez S, Randall TD (2017) Immunological functions of the omentum. *Trends Immunol* **38**, 526–536.
- Michailova KN, Usunoff KG (2004) The milky spots of the peritoneum and pleura: structure, development and pathology. *Biomed Rev* **15**, 47–66.
- Mignini F, Streccioni V, Amenta F (2003) Autonomic innervation of immune organs and neuroimmune modulation. *Auton Autacoid Pharmacol* **23**, 1–25.
- Mitchel GAG (1956) *Cardiovascular Innervation*. Edinburgh: E. & S. Livingstone Ltd.
- Olofsson PS, Rosas-Ballina M, Levine YA, et al. (2012) Rethinking inflammation: neural circuits in the regulation of immunity. *Immunol Rev* **248**, 188–204.
- Paget S (1889) Distribution of secondary growths in cancer of the breast. *Lancet* **133**, 571–573.
- Rosas-Ballina M, Olofsson PS, Ochani M, et al. (2011) Acetylcholine-synthesizing T cells relay neural signals in a vagus nerve circuit. *Science* **334**, 98–101.
- Schurink B, Cleypool CGJ, Bleys RLAW (2019) A rapid and simple method for visualizing milky spots in large fixed tissue samples of the human greater omentum. *Biotech Histochem* **21**, 1–6.
- Shimotsu M, Kawata M, Hagiwara A, et al. (1989) Milky spots in the human greater omentum: macroscopic and histological identification. *Acta Anat (Basel)* **136**, 211–216.
- Shimotsu M, Takahashi T, Kawata M, et al. (1991) Cellular subsets of the milky spots in the human greater omentum. *Cell Tissue Res* **264**, 599–601.
- Tsujimoto H, Takahashi T, Hagiwara A, et al. (1995) Site-specific implantation in the milky spots of malignant cells in peritoneal dissemination: immunohistochemical observation in mice inoculated intraperitoneally with bromodeoxyuridine-labelled cells. *Br J Cancer* **71**, 468–472.



- Tsujimoto H, Hagiwara A, Shimotsuma M, et al.** (1996) Role of milky spots as selective implantation sites for malignant cells in peritoneal dissemination in mice. *J Cancer Res Clin Oncol* **122**, 590–595.
- Van Vugt E, Van Rijthoven EA, Kamperdijk EW, et al.** (1996) Omental milky spots in the local immune response in the peritoneal cavity of rats. *Anat Rec* **245**, 235–245.
- Vida G, Peña G, Deitch EA, et al.** (2011) Alpha7-cholinergic receptor mediates vagal induction of splenic norepinephrine. *J Immunol* **186**, 4340–4346.
- Vida G, Peña G, Kanashiro A, et al.** (2017)  $\beta$ 2-Adrenoreceptors of regulatory lymphocytes are essential for vagal neuro-modulation of the innate immune system. *FASEB J* **25**, 4476–4485.
- Wijffels JF, Hendrickx RJ, Steenbergen JJ, et al.** (1992) Milky spots in the mouse omentum may play an important role in the origin of peritoneal macrophages. *Res Immunol* **143**, 401–409.
- Wilkosz S, Ireland G, Khwaja N, et al.** (2005) A comparative study of the structure of human and murine greater omentum. *Anat Embryol (Berl)* **209**, 251–261.
- Yildirim A, Aktaş A, Nergiz Y, et al.** (2010) Analysis of human omentum-associated lymphoid tissue components with S-100: an immunohistochemical study. *Rom J Morphol Embryol* **51**, 759–764.
- Zahalka AH, Arnal-Estapé A, Maryanovich M, et al.** (2017) Adrenergic nerves activate an angio-metabolic switch in prostate cancer. *Science* **358**, 321–326.